Effect of Rare Earth Doping on Magnetic Properties of Cobalt Ferrite Nanocrystals

Y. Cedeño-Mattei[*], O. Perales-Pérez[*,**], C. Osorio-Cantillo[*], and O. N. C. Uwakweh[**]

[*]Department of Chemistry, University of Puerto Rico-Mayagüez Campus, Mayagüez, PR 00681-9019
[**]Department of Engineering Science & Materials, University of Puerto Rico-Mayagüez Campus, Mayagüez, PR 00681-9044, ojuan@uprm.edu

ABSTRACT

Cobalt ferrite ($CoFe_2O_4$) is a highly anisotropic magnetic material due to the magnetocrystalline anisotropy contribution from Co^{2+}. The addition of foreign cations of different oxidation states, substituting Co^{2+} or Fe^{3+}, can lead to an atomic rearrangement in the tetrahedral and octahedral sites of the ferrite structure and, consequently, modify its magnetic properties. On that basis, bare and rare earth ions (Yb^{3+} and Gd^{3+})-doped cobalt ferrite nanocrystals have been synthesized by a modified coprecipitation method. Produced nanocrystals were characterized by X-Ray Diffraction, Vibrating Sample Magnetometry and Mössbauer Spectroscopy. Small amounts of dopant species (atomic fractions of 0.01 for Gd^{3+} or 0.007 for Yb^{3+}) caused an increase in room-temperature coercivity from 3.8 kOe (pure ferrite) up to 5.0 kOe. The attained coercivity is very close to the maximum value (5.3 kOe) predicted for this material. Mössbauer Spectroscopy suggested the presence of superparamagnetic particles in the powders. Also, the cation distribution did not show any noticeable change in both doped systems.

Keywords: cobalt ferrite, high coercivity, nanocrystals, rare earth dopants.

1 INTRODUCTION

The unusual properties displayed by cobalt-ferrite ($CoFe_2O_4$) nanoparticles enable this material to be considered for advanced technological applications, ranging from biomedical to magnetic storage. High coercivity, strong uniaxial anisotropy and a moderate magnetization are features of this type of magnetic material in addition to its high chemical stability and mechanical hardness. The high anisotropy in cobalt ferrite is attributed to the magnetocrystalline anisotropy contribution from Co^{2+} species. The addition of foreign cations of different oxidation states, substituting Co^{2+} or Fe^{3+} in the ferrite lattice, can lead to an atomic rearrangement between tetrahedral and octahedral sites and, consequently, modify its magnetic properties [1-2]. The preference of these foreign cations for a specific site (A or B) will also affect the resulting magnetic behavior. Cobalt ferrite had been doped with a variety of metal ions including Ni, Cr, Mn, Al, Zn and Cu, which clearly affected the corresponding structural and magnetic properties [3-15]. The fact that spin–orbital coupling is usually much stronger in rare-earth ions (RE) than in first row transition metal ions should also affect the magnetic properties of $CoFe_2O_4$ if RE species partially replace Fe^{3+} in the ferrite structure [16]. RE ions have been incorporated in a wide range of ferrites; for example, the incorporation of Gd^{3+} into the Mn-Zn ferrite structure helped to enhance the pyromagnetic coefficient [17] or lower its Curie temperature [18]. In the specific case of bulk cobalt ferrite, RE^{3+} (La, Ce, Nd, Sm, Gd, Tb, and Ho) dopants would cause a change in saturation magnetization due to the difference in the contributions from the magnetic moment of the substituted ion [19]. This variation in magnetization was strongly dependent on the nature of the dopant ions [16, 20]. Ferrite crystal size, size distribution, lattice distortion, and formation of isolated phases caused by the presence of RE^{3+} species, could also affect the corresponding magnetic properties [21].

On this basis and in order to investigate the effect of RE-doping on non-sintered cobalt ferrite nanocrystals, pure and rare earth ions (Yb^{3+} and Gd^{3+})-doped ferrite have been synthesized by a modified coprecipitation method. In our approach, the inhibition of crystal growth within the single domain region has been achieved through a fine control of the oversaturation conditions during the ferrite formation in water.

2 EXPERIMENTAL

2.1 Synthesis of Cobalt Ferrite Nanocrystals

Ferrite nanocrystals were synthesized by a modified coprecipitation method described in detail by Cedeño-Mattei *et al.* [22]. Suitable weigths of the precursor salts were used to keep the Co/M mole ratio, (M= Fe and Yb or Gd species) according to $CoFe_{2-x}RE_xO_4$ stoichiometry. In the modified approach, the control of the solution oversaturation conditions was attained by a precise monitoring of the flow-rate of the addition of metals solution into boiling NaOH under suitable synthesis conditions [23].

2.2 Nanocrystals Characterization

Dried nanocrystals were submitted to characterization by X-ray Diffractometry (XRD), Vibrating Sample

Magnetometry (VSM) and Mössbauer Spectroscopy techniques. The average crystallite size of powders was estimated by the Scherrer's equation for the (440) XRD reflection. The maximum external magnetic field for M-H measurements was 2.2T. VSM and Mössbauer measurements were conducted under room-temperature conditions. Mössbauer spectroscopic measurements were carried out with a WEBRES spectrometer operating in the transmission mode, with a 50 mCi ^{57}Co source in a Rh matrix from Ritverc, GmbH. The velocity scale calibration was done with known line positions of α-Fe iron metal foil. The 1024-point raw data were folded and analyzed using WMOSS. A hyperfine field distribution model was used in the spectral fitting.

3 RESULTS AND DISCUSSION

3.1 XRD Analyses

All samples were synthesized for one hour of reaction and using a 0.34 M NaOH aqueous solution. The solution containing Co^{2+}, Fe^{3+} and Gd^{3+} or Yb^{3+} ions was added into the NaOH one at 1mL/min, 5mL/min or 10mL/min. For comparison purposes, doped-Cobalt ferrite powders were also synthesized with no control of the flow-rate. The atomic fraction of the dopants ranged from 0.007 to 0.07 for Yb, and from 0.01 to 0.10 for Gd species. Figure 1 shows the XRD patterns for the solids produced at different flow-rates of reactants addition and Yb atomic fraction, 'x', 0.07. Although most of the peaks corresponded to the ferrite structure, additional peaks at 2θ values of 32° and 45°, attributed to the (321) and (431) planes in Yb_2O_3, were also detected. These peaks were not observed for 'x' values below 0.07, suggesting the actual incorporation of the Yb species into the ferrite lattice. XRD patterns corresponding to Gd-doped cobalt ferrite showed no evidence of formation of any crystalline impurity phase even at a Gd atomic fraction as high as 0.10.

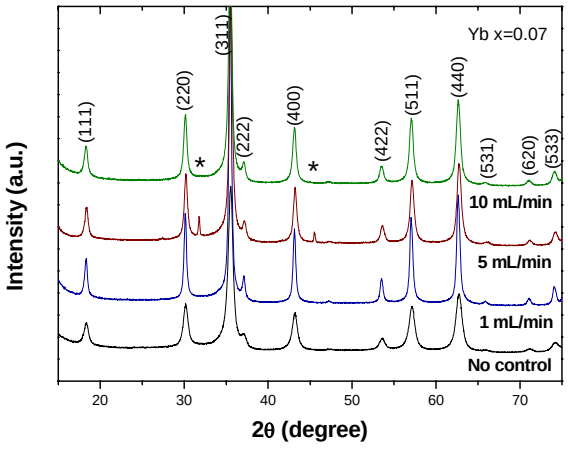

Figure 1: XRD patterns for Yb-doped cobalt ferrite powders synthesized at different flow rates. The dopant atomic fraction was 'x' = 0.007.

[Yb] atomic fraction	Flow Rate (mL/min)	t (nm)	a (Å)	H_c (Oe)	M_{max} (emu/g)
x = 0.007	No control	10.45	8.365	360	62
	1	18.32	8.383	4963	55
	5	14.99	8.392	1893	59
	10	14.27	8.385	1766	59
x = 0.04	No control	10.52	8.373	306	56
	1	19.67	8.391	4890	52
	5	16.44	8.389	1622	57
	10	14.24	8.390	1129	58
x = 0.07	No control	10.55	8.384	308	51
	1	18.34	8.390	2170	51
	5	15.94	8.386	1676	51
	10	15.32	8.379	1055	52

[Gd] atomic fraction	Flow Rate (mL/min)	t (nm)	a (Å)	H_c (Oe)	M_{max} (emu/g)
x = 0.01	No control	10.04	8.373	402	61
	1	17.91	8.385	4918	53
	5	15.45	8.394	2503	57
	10	14.18	8.383	1782	54
x = 0.05	No control	10.63	8.379	411	52
	1	17.92	8.388	3493	47
	5	16.05	8.385	2287	54
	10	14.68	8.382	1421	54
x = 0.10	No control	10.66	8.381	436	46
	1	19.41	8.381	3603	38
	5	16.18	8.388	2020	47
	10	13.60	8.383	1411	46

Table 1: Summary of the structural and magnetic properties of Yb and Gd-doped cobalt ferrite nanocrystals.

Table 1 shows the average crystallite size, 't', and lattice parameter, 'a', values determined from XRD measurements for all synthesized samples. In this table, 'no-control' means the reactants were mixed without any control on flow-rate. The ferrite lattice parameter for pure cobalt ferrite synthesized at 1mL/min was estimated at 8.383 Å, which is in good agreement with the bulk value of 8.377 Å. The corresponding average crystallite size was 15.50 nm. In general, the average crystallite size of both Yb- and Gd-doped cobalt ferrite increased when they were synthesized under particular flow-rate controlled conditions. For the Gd(0.01)-cobalt ferrite sample, the average crystallite size varied from 10 nm, with no control on flow-rate, up to 18 nm when the flow-rate was 1 mL/min. Flow-rates higher than 1 mL/min caused the average crystallite size to drop. A similar trend was noticed for the Yb-doped nanocrystals. Lower flow-rates should have favored heterogeneous nucleation, where earlier nuclei should have acted as pre-existent seeds and hence, promoted crystal growth in both doped systems. On the contrary, the rise of the flow-rate would have enhanced the rate of homogeneous nucleation, which can explain the reduction in crystal size.

NSTI-Nanotech 2009, www.nsti.org, ISBN 978-1-4398-1782-7 Vol. 1, 2009

3.2 VSM Measurements

The magnetic characterization results for investigated ferrite nanocrystals are also summarized in Table 1. M-H measurements confirmed the strong influence of the synthesis conditions on the magnetic properties of the ferrite nanocrystals; in particular, the coercivity was drastically enhanced when the crystals were formed under controlled flow-rate conditions. As figure 2 shows, the coercivity for the cobalt ferrite doped with Yb (x = 0.007) was increased from 360 Oe, (no control on flow rate), up to 5.0 kOe (1mL/min). In turn, the coercivity varied from 402 Oe (no control on flow rate) to 4.9 kOe (1mL/min) when the ferrite was synthesized with a Gd atomic fraction of 0.01. The maximum magnetization for these high-coercivity Yb- and Gd-doped samples was 55 and 52 emu/g, respectively. Pure, i.e. undoped, cobalt ferrite synthesized under the same conditions reported coercivity and saturation magnetization values of 3.8 kOe and 57 emu/g, respectively. The rise in coercivity could be attributed to the strong spin-orbital coupling of the RE ions incorporated in the ferrite lattice, for small dopant concentrations. However, this increase in coercivity can also be a consequence of crystal growth within the single domain region promoted by low flow-rates, as suggested by XRD analyses. Furthermore, the coercivity of the rare-earth doped ferrites (around 5.0 kOe) is very close to the maximum theoretical value (5.3 kOe) predicted for a system of non interacting single domain cobalt ferrite particles with cubic anisotropy [24]. For the Yb^{3+} doped cobalt ferrite, the presence of paramagnetic Yb_2O_3 (x > 0.04) can explain the drop in both, the saturation magnetization and coercivity.

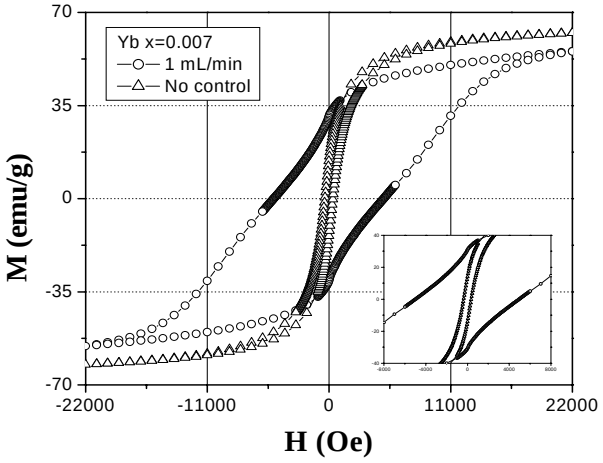

Figure 2: M-H loops at 300K for Yb-doped cobalt ferrite synthesized with (1 mL/min) and without control on flow-rate. The dopant atomic fraction was 'x' = 0.007. The inset shows the M-H data around the origin.

3.3 Mössbauer Spectroscopy

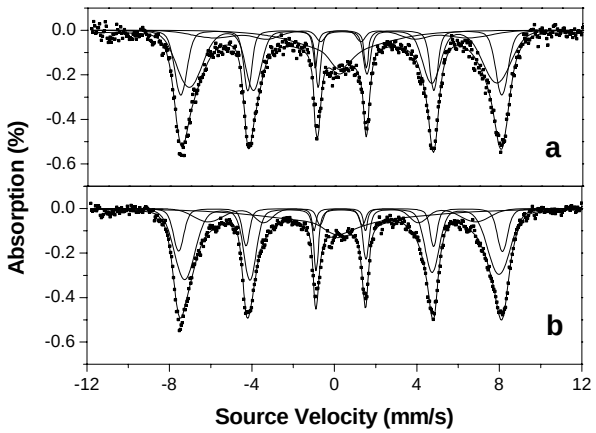

Figure 3: Mössbauer spectra of $CoFe_2O_4$ doped with: (a) Gd, ('x'= 0.007) and (b) Yb, ('x'= 0.01). Fitted spectra show the corresponding sub-sites: three magnetically ordered site, and a paramagnetic site. Both samples were synthesized at 1 mL/min.

The Mössbauer spectra of the Gd- and the Yb-doped $CoFe_2O_4$ samples (Figures 3) were characterized by prominent sextets while the central portion of the spectra showed distinct doublet peaks associated with superparamagnetic particles. This feature of the profile suggests that all the particles may have not been of the same size with most of them displaying the magnetic order evidenced by the sextets. Moreover, careful examination of the superimposed spectra showed that there were slightly more of these superparamagnetically relaxed particles in the Yb^{3+} doped powder than in the Gd-doped one.

Mössbauer data were originally fitted with five Fe-sites: four corresponding to the magnetically ordered particles and one attributed to the small portion of superparamagnetically relaxed particles. The first sub site yielded a zero relative intensity, or very insignificant amount, which therefore led to the refitting of the spectra with four sites as shown in Figure 3-a (Gd-doped ferrite). The first site yielded a hyperfine internal magnetic field of 481.13 kOe, with a relative abundance of 24.8 %. The hyperfine internal magnetic fields for the second and third sites were 461.14 kOe and 401.46 kOe, respectively, with corresponding relative abundances of 42.1 %, and 18.6 %. The central portion corresponding to the non-magnetically ordered particles accounted for 18.6% of the total material. For the Yb-doped $CoFe_2O_4$, (Figure 3-b), the first site yielded a hyperfine internal magnetic field of 485.67 kOe, with a relative abundance of 15.94%. The hyperfine internal magnetic fields for the second and third sites were 470.99 kOe and 398.66 kOe, respectively, with corresponding relative abundances of 50.55% and 12.71%. The central portion of the spectrum yielded a paramagnetic

order accounting for 20.72% of the entire material. Given the minimal difference between these two spectra, it can be suggested that the Fe sites were similarly altered at the doping Gd^{3+} and Yb^{3+} levels quoted in this study. In both cases, the superparamagnetic component at the central portion of the spectra accounted for no more than 21% of the total phases. A detailed analysis of this non-magnetically ordered component would be better resolved after further work at additional doping levels.

4 CONCLUDING REMARKS

RE-doped cobalt ferrite nanocrystals, ranging from 10 to 20 nm, have been synthesized. The coercivity of the rare-earth doped ferrites was very close to the maximum theoretical value (5.3 kOe) when low flow-rates of addition of reactants were used. Mössbauer measurements of the Gd^{3+} and Yb^{3+} doped ferrites showed that the non-magnetically ordered portion accounted for 18.6% and 20.72% of the total material, respectively. Therefore, any difference detected in the coercivity values of the samples could be associated with the difference between the relative amounts of superparamagnetically relaxed particles in them.

5 ACKNOWLEDGMENTS

This material is based upon work supported by the National Science Foundation under NSF-PREM Grant No. 0351449 at UPRM. The authors also acknowledge the support provided by the NSF-EPSCoR Institute for Functional Nanomaterials (IFN).

REFERENCES

[1] B. H. Liu and J. Ding Appl. Phys. Lett., 88, 042506, 2006.
[2] S. D. Bahme and P. A. Joy J. Appl. Phys., 100, 113911, 2006.
[3] F. Zhang, Y. Kitamoto, M. Abe, and M. Naoe J. Appl. Phys., 87, 6881, 2000.
[4] K. Krieblea, C. C. H. Lo, Y. Melikhov, and J. E. Snyder, J. Appl. Phys., 99, 08M912, 2006.
[5] M. J. Iqbal and M. R. Siddiquah J. Alloys Compd., 453, 513, 2008.
[6] K. Krieblea, T. Schaeffer, J. A. Paulsen, A. P. Ring, C. C. H. Lo, and J. E. Snyder J. Appl. Phys., 97, 10F101, 2005.
[7] O. Caltun, G. S. N. Rao, K. H. Rao, B. P. I. Dumitru, C.-O Kim, and C. Kim J. Magn. Magn. Mater., 316, e618, 2007.
[8] S. D. Bhame and P. A. Joy J. Appl. Phys., 100, 113911, 2006.
[9] S. D. Bhame and P. A. Joy J. Appl. Phys., 99, 073901, 2006.
[10] K. J. Kim, H. K. Kim, and J. Y. Park J. Magn. Magn. Mater., 304, e106, 2006.
[11] S. J. Kim, B. R. Myoung, and C. S. Kim J. Appl. Phys., 93, 7504, 2003.
[12] S. Singhal, S. K. Barthwal, and K. Chandrac J. Magn. Magn. Mater., 306, 233, 2006.
[13] S. W. Lee, Y. G. Ryu, and K. J. Yang, S. Y. An, and C. S. Kim J. Appl. Phys., 91, 7610, 2002.
[14] G.V. Duong, N. Hanh, D.V. Linh, R. Groessinger, P. Weinberger, E. Schafler, and M. Zehetbauer J. Magn. Magn. Mater., 311, 46, 2007.
[15] C. Venkateshwarlu, and D. Ravinder J. Alloys Compd., 426, 4, 2006.
[16] L. B. Tahar, M. Artus, S. Ammarb, L. S. Smiri, F. Herbst, M.-J. Vaulay, V. Richard, J.-M. Grenèche, F. Villain, and F. Fiévet J. Magn. Magn. Mater., 320, 3242, 2008.
[17] R. V. Upadhyay, R. V. Mehta, K. Parekh, D. Srinivas, and R. P. Pant J. Magn. Magn. Mater., 201, 129, 1999.
[18] T. N. Brusentsova, N. A. Brusentsov, V.D. Kuznetsov, and V.N. Nikiforov J. Magn. Magn. Mater., 293, 298, 2005.
[19] O. Caltuna, I. Dumitru, M. Feder, N. Lupu, and H, .Chiriac J. Magn. Magn. Mater., 320, e869, 2008.
[20] L. B. Tahar, L. S. Smiri, M. Artus, A.-L. Joudrier, F. Herbst, M.J. Vaulay, S. Ammar, and F. Fiévet Mat. Res. Bull., 42, 1888, 2007.
[21] M. M. Rashad, R. M. Mohamed, H. El-Shall J. Mater. Proc. Tech., 198, 139,2008.
[22] Y. Cedeño-Mattei, O. Perales-Perez, M. S. Tomar, F. Roman, P. M. Voyles, and W. G. Stratton J. Appl. Phys., 103, 07E512, 2008.
[23] Y. Cedeño-Mattei, O. Perales-Pérez Microelectron. J., In Press, 2008.
[24] E. W. Lee and J. E. Bishop, Proc. Phys. Soc., 89, 661, 1966.